

SOLVOTHERMAL SYNTHESIS OF Bi_2WO_6 AND ITS PHOTOCATALYTIC ACTIVITY UNDER VISIBLE LIGHT IRRADIATION

Trinh Duy Nguyen^{1,*}, Van Thi Thanh Ho², Long Giang Bach¹

¹NTT Institute of High Technology, Nguyen Tat Thanh University, 298-300A, Nguyen Tat Thanh, Ho Chi Minh City, Vietnam

²Hochiminh City University of Natural Resources and Environment, Vietnam

*Email: nguyenduytrinh86@gmail.com

Received: 15 August 2016; Accepted for publication: 10 November 2016

ABSTRACT

Flower-like Bi_2WO_6 were successfully synthesized using the solvothermal method at different temperatures and characterized by XRD, FE-SEM, and DRS. We also investigated the photocatalytic activity of Bi_2WO_6 for the decomposition of rhodamine B under visible light irradiation. From XRD and SEM results, the reaction temperature has significant effects on the morphologies of the samples. From DRS results, Bi_2WO_6 samples displayed the absorption spectrum up to the visible region and then they showed the high photocatalytic activity under visible light irradiation, as a comparison with TiO_2 -P25.

Keywords: Bi_2WO_6 , solvothermal method, rhodamine B, visible light irradiation.

1. INTRODUCTION

Bismuth tungstate (Bi_2WO_6), an Aurivillius-phase perovskite, has been extensively used in photocatalytic applications [1 - 3]. Bi_2WO_6 is a typical n-type direct band gap semiconductor with a band gap of 2.75 eV, and thus it exhibits high photooxidative capacity as a catalyst for water splitting processes and degradation of organic pollutions under visible light irradiation [1]. It is a well-known fact that Bi_2WO_6 has two types of crystal structures: orthorhombic (space group $B2cb$, with $a = 5.457$, $b = 5.436$, $c = 16.427\text{\AA}$, $Z = 4$) and monoclinic (space group structure. Monoclinic structure existed at a high-temperature phase ($> 960\text{ }^\circ\text{C}$) while orthorhombic structures existed at a low and intermediate temperatures ($< 960\text{ }^\circ\text{C}$) [4 - 6]. However, the orthorhombic phase was usually employed for the presently studied Bi_2WO_6 photocatalyst. In the photocatalytic process of TiO_2 and another semiconductor, the main active species is $\bullet\text{OH}$. However, Bi_2WO_6 cannot generate $\bullet\text{OH}$ in the photocatalytic process. The main active species were reported to be photogenerated holes (h^+), conduction band electrons (e_{CB}^-) and superoxide radical ($\text{O}_2\bullet^-$) [3, 7 - 9].

In our study, Bi_2WO_6 photocatalyst was synthesized by solvothermal method. The effects of temperature reaction on morphologies were investigated. We also investigated the

photocatalytic activity of Bi₂WO₆ in the decomposition of rhodamine B (RhB) under visible light irradiation.

2. MATERIALS AND METHODS

All chemicals were used as received without further purification and analytical grade. The syntheses of Bi₂WO₆ photocatalysts were prepared using a solvothermal method in the mixed solvent of ethylene glycol monomethyl ether (EGME) and water. Typically, Bi(NO₃)₃ (5 mmol, 2.475 g) was dissolved in 50 mL EGME. A solution of Na₂WO₄·H₂O (2.5 mmol, 0.833 g) in 50 mL H₂O was added into the above solution. The mixture was stirred for 1 h before being transferred into a Teflon-lined stainless steel autoclave and heated at 160-240 °C for 12 h. After each the reaction, the obtained suspension was centrifuged at 10000 rpm for 10 minutes, and the Bi₂WO₆ solids at the bottom of the tube were rinsed with water and ethanol for five times, dried at 60 °C overnight, calcined at 300 °C in air for 3 h.

The crystal phase was examined by powder X-ray diffraction (XRD) patterns with Cu K α radiation (Rigaku Co. Model DMax). Surface morphologies of the products were observed by scanning electron microscopy (SEM, JEOL JSM6700F) at an accelerating voltage of 3 kV. The optical properties of the products were recorded on a Varian Cary 100 UV-vis spectrophotometer using polytetrafluoroethylene (PTFE) as a standard.

Photocatalytic activities of the samples were calculated by the photocatalytic decomposition of RhB under visible region with a 300 W Xe-arc lamp (Oriol) and a 410 nm cut-off filter. The light was passed through a 10 cm IR water filter and then focused onto a 150 mL Pyrex with a quartz window. In all catalytic activity of experiments, the reactor was filled with a mixture of RhB aqueous solution (10⁻⁵ M, 100 mL) and the given photocatalyst (100 mg). Before lighting on, the solution was magnetically stirred in the dark for 60 minutes to establish adsorption-desorption equilibrium between the photocatalyst surface and organic molecules. At given time intervals, 3 mL of the suspension was withdrawn and then filtered through a 0.22 μ m membrane filter to get the clear solution. A decrease in the concentration of RhB solution was measured with a UV-vis spectrophotometer (Mecasys Optizen Pop) at $\lambda = 554$ nm.

3. RESULTS AND DISCUSSION

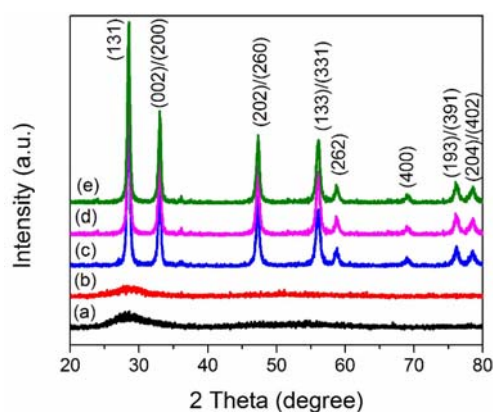


Figure 1. XRD patterns of Bi₂WO₆ samples prepared with different synthesis temperatures: room temperature (a), 160 °C (b), 180 °C (c), 200 °C (d), and 240 °C (e).

XRD patterns of the as-synthesized Bi_2WO_6 samples prepared at different temperatures are shown in Figure 1. In the first stage of the reaction, when we added the WO_4^{2-} solution to the Bi^{3+} solution, a white precipitate was rapidly formed. From the XRD result (Figure 1(a)), we conclude that the starting precipitate mostly had an amorphous phase. The amorphous phase was transformed into the orthorhombic Bi_2WO_6 after the 12 hours of the solvothermal process. However, when the reaction temperature was 160 °C, the XRD peaks are indexed to an amorphous state (Figure 1(b)) and thus Bi_2WO_6 could not be formed. After increasing the reaction temperature up to 180 °C, all the XRD peaks are well indexed to orthorhombic Bi_2WO_6 (JCPDS No. 73-1126) [4, 5, 10, 11]. No peak for tungsten oxide and bismuth oxide phase or other impurities were detected, which indicated the high purity of the product.

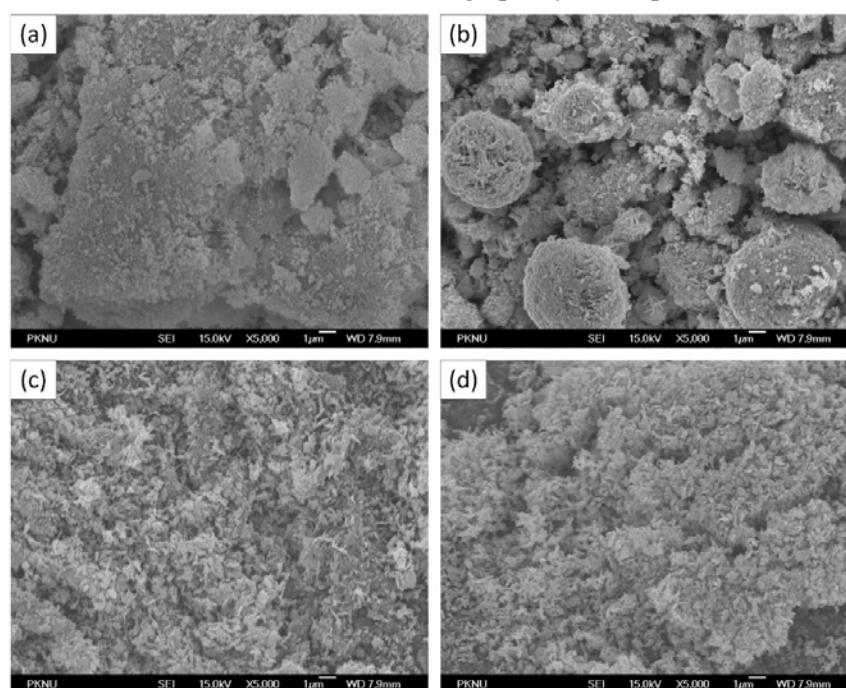


Figure 2. SEM images of Bi_2WO_6 samples prepared with different synthesis temperatures: 160 °C (a), 180 °C (b), 200 °C (c), and 240 °C (d).

The morphologies of the as-prepared Bi_2WO_6 were examined by SEM analysis and the results are shown in Figure 2. As shown in Figure 2, when the sample was treated at a lower temperature, the amorphous phase was observed. As the reaction temperature increased to 180 °C, flower-like Bi_2WO_6 super structure formed. As the reaction temperature extended to 200 and 240 °C, aggregates of Bi_2WO_6 nanoparticles were produced. From these images, we can come to a conclusion that the reaction temperature has significant effects on the morphologies of the samples.

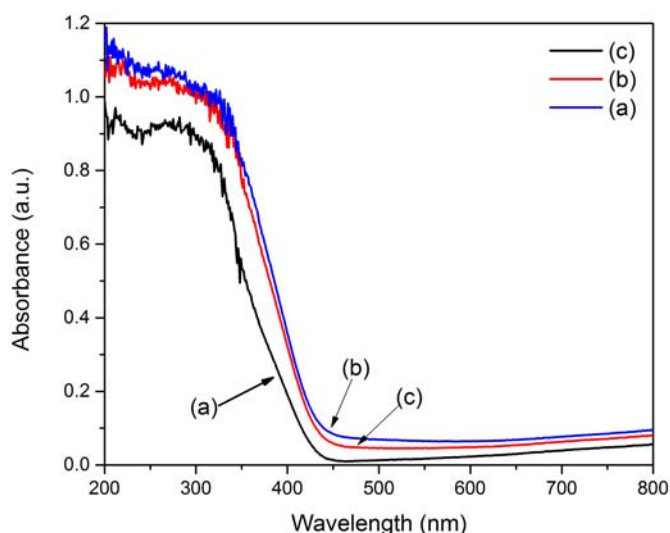


Figure 3. UV-vis DRS of Bi_2WO_6 catalysts prepared using different synthesis temperatures: 180 °C (a), 200 °C (b) and 240 °C (c).

The light absorption properties of the photocatalysts were examined using UV–vis diffuse reflectance spectroscopy. Figure 3 shows the UV–vis DRS of the Bi_2WO_6 samples prepared at different synthesis temperatures. As shown in Figure 3, the spectra of Bi_2WO_6 samples showed intensive absorption bands in the visible light region. This result suggests that Bi_2WO_6 samples can be used as potential visible-light-driven photocatalysts. The indirect band gap energy (E_g) of all samples were determined from the tangent line in the plots of the modified Kubelka–Munk function $[F(R_\infty)/\text{h}\nu]^{1/2}$ versus photon energy. The band gap values of the various samples are shown in Table 1. The band gap of Bi_2WO_6 nanoparticles is shifted from 2.81 to 2.86 eV.

Table 1. The physical properties and photocatalytic activity of the as-prepared samples.

No	Sample	Solvothermal temperature (°C)	S_{BET} (mg/m^2)	E_g (eV)	k ($\times 10^{-3} \text{min}^{-1}$)
1	P-25 TiO_2	-	-	3.2	1.8
2	Bi_2WO_6	Room temperature	-	-	2.1
3	Bi_2WO_6	160	-	-	0.7
4	Bi_2WO_6	180	322.413	2.81	10.7
5	Bi_2WO_6	200	252.565	2.82	8.3
6	Bi_2WO_6	240	203.337	2.86	6.4

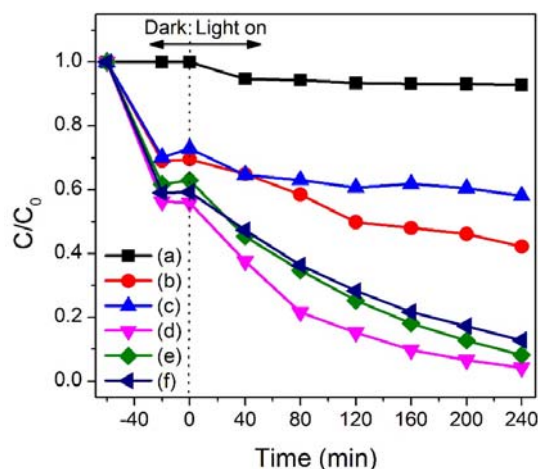


Figure 4. Variation of RhB concentration against irradiation time using Bi_2WO_6 samples prepared using different synthesis temperatures: room temperature (b), $160\text{ }^\circ\text{C}$ (c), $180\text{ }^\circ\text{C}$ (d), $200\text{ }^\circ\text{C}$ (e) and $240\text{ }^\circ\text{C}$ (f), and without catalyst under visible light (a).

The photocatalytic activity for the decomposition of RhB on P-25 TiO_2 and Bi_2WO_6 samples prepared at different reaction temperatures under visible light irradiation is shown in Figure 4. The photodecomposition rate constant (k) of RhB over samples, as calculated from a pseudo-first order reaction kinetic model: $\ln(C_0/C) = kt$. The results are reported in Table 1. When a blank test was carried out in the absence of the photocatalyst, about 1 % of the RhB was decomposed after 240 min by the photolysis reaction. As shown in Figure 4 and Table 1, Bi_2WO_6 catalysts showed higher photocatalytic activity compared to P-25 TiO_2 catalyst. It is well known that the photocatalytic activity is related to the photoabsorption. Especially, this photocatalytic decomposition of RhB is carried out under visible light irradiation. Therefore, the amount of photo absorption in the visible region plays an important role on the photocatalytic activity. As shown in Figure 3, the spectra of Bi_2WO_6 samples showed intensive absorption bands in the visible light region and the higher photocatalytic activity. Moreover, Bi_2WO_6 catalyst at $180\text{ }^\circ\text{C}$ showed the highest photocatalytic activity. It is thought that this photocatalytic reaction has a high surface area effect, wherein the photocatalytic activity increases with an increase of surface area.

4. CONCLUSIONS

We have prepared Bi_2WO_6 using the solvothermal method at different temperatures. The phase structure and morphology of as-prepared Bi_2WO_6 samples were characterized by XRD, SEM, and DRS. We have also investigated the photocatalytic activity of these materials for the decomposition of RhB under visible light irradiation. From DRS results, Bi_2WO_6 samples showed the absorption spectrum up to the visible region and then their photocatalytic activity was shown higher than commercial P-25 TiO_2 materials. Bi_2WO_6 sample prepared at $180\text{ }^\circ\text{C}$ showed the highest photocatalytic activity due to high surface area effect.

Acknowledgements. This research is funded by Foundation for Science and Technology Development Nguyen Tat Thanh University, Ho Chi Minh City, Vietnam.

REFERENCES

1. Zhou L., Yu M., Yang J., Wang Y., Yu C. - Nanosheet-based Bi₂Mo_xW_{1-x}O₆ solid solutions with adjustable band gaps and enhanced visible-light-driven photocatalytic activities, *J. Phys. Chem. C*. **114** (2010) 18812–18818.
2. Wu L., Bi J., Li Z., Wang X., Fu X. - Rapid preparation of Bi₂WO₆ photocatalyst with nanosheet morphology via microwave-assisted solvothermal synthesis, *Catal. Today*. **131** (2008) 15–20.
3. Pope T. R., Lassig M. N., Neher G., Weimar III R. D., Salguero T. T. - Chromism of Bi₂WO₆ in single crystal and nanosheet forms, *J. Mater. Chem. C*. **2** (2014) 3223.
4. Maczka M., Fuentes A. F., Kepiski L., Diaz-Guillen M. R., Hanuza J. - Synthesis and electrical, optical and phonon properties of nanosized Aurivillius phase Bi₂WO₆, *Mater. Chem. Phys.* **120** (2010) 289–295.
5. Wolfe R. W., Newnam R. E., Kay M. I. - Crystal structure of Bi₂WO₆, *Solid State Commun.* **7** (1969) 1797–1801.
6. Wolfstieg U., Macherauch E. - New Text Document, *Hiirterei-Tech. Mitt.* **31** (1976) 2.
7. Fu H., Pan C., Yao W., Zhu Y. - Visible-light-induced degradation of rhodamine B by nanosized Bi₂WO₆, *J. Phys. Chem. B*. **109** (2005) 22432–22439.
8. Chen P., Zhu L., Fang S., Wang C., Shan G. - Photocatalytic Degradation Efficiency and Mechanism of Microcystin-RR by Mesoporous Bi₂WO₆ under Near Ultraviolet Light, *Environ. Sci. Technol.* **46** (2012) 2345–2351.
9. Ding X., Zhao K., Zhang L. - Enhanced Photocatalytic Removal of Sodium Pentachlorophenate with Self-Doped Bi₂WO₆ under Visible Light by Generating More Superoxide Ions, *Environ. Sci. Technol.* **48** (2014) 5823–5831.
10. Zhang L., Wang H., Chen Z., Wong P.K., Liu J. - Bi₂WO₆ micro/nano-structures: Synthesis, modifications and visible-light-driven photocatalytic applications, *Appl. Catal. B Environ.* **106** (2011) 1–13.
11. Sun S., Wang W., Zhang L. - Facile preparation of three-dimensionally ordered macroporous Bi₂WO₆ with high photocatalytic activity, *J. Mater. Chem.* **22** (2012) 19244–19249.